EFDA–JET–CP(14)01/06

B. Bazylev, G. Arnoux, J.W. Coenen, G.F. Matthews, S. Jachmich,
I. Balboa, M. Clever, R. Dejarnac, I. Coffey, Y. Corre, S. Devaux,
L. Frassinetti, E. Gauthier, J. Horacek, M. Knaup, K. Krieger,
S. Marsen, A. Meigs, Ph. Mertens, R.A. Pitts, T. Puetterich,
M. Rack M. Stamp, G. Sergienko, P. Tamain, V. Thompson,
and JET EFDA contributors

MEMOS Code Validation on JET Transient Tungsten Melting Experiments

MEMOS Code Validation on JET Transient Tungsten Melting Experiments

B. Bazylev[1,2], G. Arnoux[1,3], J.W. Coenen[1,4], G.F. Matthews[1,3], S. Jachmich[1,5], I. Balboa[1,3], M. Clever[1,4], R. Dejarnac[1,6], I. Coffey[1,7], Y. Corre[1,8], S. Devaux[1,3], L. Frassinetti[1,9], E. Gauthier[1,8], J. Horacek[1,6], M. Knaup[1,4], K. Krieger[1,10], S. Marsen[1,11], A. Meigs[1,3], Ph. Mertens[1,4], R.A. Pitts[1,12], T. Puetterich[1,10], M. Rack[1,4], M. Stamp[1,3], G. Sergienko[1,4], P. Tamain[1,8], V. Thompson[1,3], and JET EFDA contributors*

JET-EFDA, Culham Science Centre, OX14 3DB, Abingdon, UK

[1]JET-EFDA, Culham Science Centre, Abingdon OX14 3DB, UK
[2]Karlsruhe Institute of Technology, P.O.Box 3640, D-76021 Karlsruhe, Germany
[3]Culham Centre for Fusion Energy, Abingdon
[4]IEK-4, Forschungszentrum Jülich GmbH, Partner in the Trilateral Euregio Cluster, Juelich, Germany
[5]Laboratory for Plasma Physics, Ecole Royale Militaire/Koninklijke Militaire School
[6]Institute of Plasma Physics AS CR, Za Slovankou 3, 18221 Praha 8, Czech Republic
[7]Astrophysics Research Centre, School of Mathematics and Physics, Queen's Univ. Belfast, UK
[8]CEA, IRFM, F-13108 Saint-Paul-lez-Durance, France
[9]Division of Fusion Plasma Physics, KTH, SE-10044 Stockholm, Sweden
[10]Max-Planck-Institut für Plasmaphysik, 85748 Garching, Germany
[11]Max-Planck-Institut für Plasmaphysik, Teilinsitut Greifswald, D-17491 Greifswald, Germany
[12]ITER Organization, Route de Vinon sur Verdon, 13115 Saint-Paul-lez-Durance, France
** See annex of F. Romanelli et al, "Overview of JET Results", (24th IAEA Fusion Energy Conference, San Diego, USA (2012)).*

Preprint of Paper to be submitted for publication in Proceedings of the
21st International Conference on Plasma Surface Interactions, Kanazawa, Japan
26th May 2014 – 30th May 2014

ABSTRACT

The ITER Organization has recently decided to install a full-tungsten (W) divertor from the start of operations. One of the key issues with such a strategy is the possibility of W melting and melt splashing during transients, which can lead to modifications of surface topology.

A new experiment was now performed on JET-ILW, in which a deliberately misaligned W element (lamella) in the outer divertor was used to perform controlled ELM transient melting experiments in a tokamak. This paper reports on the application of the 3D-MEMOS code to modeling of these experiments. Input heat loads are obtained from experimental data. The code indicates that that shielding by the evaporated tungsten prevents bulk melting. The simulations are also able to quantitatively reproduce the dimensions of the damaged area observed by high resolution photography after the first pulse in which melting was achieved

1. INTRODUCTION

The ITER Organization (IO) has recently decided to install a full-tungsten (W) divertor from the start of operations [1]. One of the key issues with such a strategy is the possibility of W melting and melt splashing during transients, which can lead to modifications of surface topology [1,2] and which may lead to higher disruption frequency or compromise subsequent plasma operation. Although every effort will be made to avoid leading edges, ITER plasma stored energies are sufficient that transients can drive shallow melting on the top surfaces of plasma-facing components (PFC) [1].

Experiments designed to investigate plasma transient heat load damage of ITER-like W targets have traditionally been performed in QSPA plasma gun facilities [3], in which the transient plasma pulse pressure significantly exceeds the values attainable in tokamaks, including ITER, and the melt motion dynamics are determined by the tangential friction force of the impacting plasma. A new experiment has now been performed on JET in the new ITER-Like Wall (ILW) environment, in which a deliberately misaligned W element (lamella) in the outer divertor has been used to perform controlled ELM transient melting experiments for the first time in a tokamak [4]. The 3D MEMOS code [5] is applied to modelling of these experiments. This is an important validation exercise on real tokamak data for a code which is being used extensively to predict melt damage on the ITER divertor [1].

Simulations are performed first for L-mode plasma loads, without the complication of ELMs, and have been performed both for a reference, well aligned lamella and the misaligned element. Input heat loads are obtained from experimental data, notably high resolution infra-red (IR) thermography [6]. During ELMing H-mode, the calculated time dependent, 3D temperature distributions in the special lamella lead to extremely high temperature gradients at the leading edge ($\sim 10^6$K/m) and noticeable W evaporation. In fact, the simulations demonstrate that consistency with the measured IR temperatures is only possible if the impinging heat flux is about a factor (fudge factor) $f_s \sim 2$–4 lower than expected from geometrical considerations [6]. The code also indicates that that shielding by the evaporated tungsten prevents bulk melting between ELMs due to significant decrease of

the surface temperature maximum during the ELMs. Encouragingly, the simulations are also able to quantitatively reproduce the dimensions of the damaged area observed by high resolution photography after the first pulse in which melting was achieved. The principle mechanism responsible for the melti motion damage is identified as the jxB force due to the thermo-emission currents from the hot surface, which generate velocities up to 1.5m/s in the central molten region and up to 0.5m/s at the periphery in the direction observed experimentally. No melt splashing is expected on the basis of the MEMOS simulations of melt depth and melt velocity.

2. HEAT LOAD SPECIFICATIONS IN THE JET-ILW EXPERIMENTS AND THE MEMOS MODELING.

The scheme of the experiments in JET-ILW is well described the ref. [4]: The outer JET divertor is split up in four so-called Stacks (A,B,C,D). In the stack A the special lamella was installed to allow significant preheating due to the front surface being exposed to the parallel heat flux Q_s in addition to the heat flux Q_n impacting to the top surface of the special lamella (Figure 1). The Q_s and Q_n are connected via geometric factor η which should be between 25 and 35 [4,6] ($Q_s = \eta Q_n$).The exposure to the parallel heat flux is achieved by producing a chamfered leading edge of 0.25–2.5mm and also lowering of the 8 lamellas in front of the exposed. The lamella has a poloidal extent of 5.9cm and is 5.5mm wide toroidally. The adequate 3D geometry of the special lamella exposure installed into the code 3D MEMOS is demonstrated on the Figure 1. All sizes of experimental conditions are fully reproduced in the 3D MEMOS target geometry. As it was in the JET-ILW experiment: angle between B and surface has to be ~ 2.5°, B = 2.87T, pressure of impacting plasma at the leading edge surface estimated from the pedestal data: ~ 6kPa in maximum of ELM and 0.01kPa in between ELMs with pressure shape corresponding to ELM shape, temperature of impacting plasma is taken about 400eV for ELMs. Due to rather high tungsten temperature achieved at the leading edge thermo-emission current J (Richardson-Dushman law) from the special lamella can appear during the ELMs that lead to action of the JxB force inside the melted tungsten. As it was observed in the TEXTOR experiments [2] in which it was found that the melt motion is generated by the thermo-emission current. This force is directed along the leading edge in poloidal direction. Simulation will be perform for the JET-ILW H-mode shot JET Pulse No: 84779 with 51 ELMs during the special lamella exposure. . Input heat loads for the 3D MEMOS simulations are obtained from experimental data, notably high resolution infra-red (IR) thermography [6]. Time dependence of Q_s along poloidal coordinate of special lamella is demonstrated on Figure 2.

3. NUMERICAL MODEL OF THE CODE 3D MEMOS

The magnitude of roughness after multiple ELMs with the heat loads over the target surface is simulated applying the fluid dynamics code 3D MEMOS [5,7,8]. The motion of melted material along the surface is described in the 'shallow water' approximation of the Navier-Stokes equations [9], with the surface tension, viscosity of molten metal, and the radiative losses from the hot surface

taken into account. The plasma pressure gradients along the divertor plate, as well as the gradient of surface tension and the JxB force of the currents (external and thermo-emission) crossing the melt layer immersed in a strong magnetic field, produce the melt acceleration.

For a derivation of the mathematical model the following assumptions are used here: the thickness of the melt layer is much smaller than the sizes of the molten layer and pressure gradients across the melt layer are absent. Therefore a velocity component parallel to the surface exists only and a melt velocity averaged over the molten layer can be used for description of the melt motion. In this case the "shallow water" approximation can be applied for the mathematical description of the melt motion. The fluid is assumed to be incompressible. Temperature dependent thermo-physical data are used.

The base system of Navier-Stocks equations together with the heat conductivity equation describe the parameters of molten W layer and heat diffusion towards solid material

$$\mathrm{div}\,\mathbf{v} = 0 \tag{1}$$

$$\rho\left(\frac{\partial \mathbf{v}}{\partial t} + \mathbf{v}\nabla\mathbf{v}\right) = -\,\mathrm{grad}\,p + \mu\,\Delta\mathbf{v} + F_L \tag{2}$$

$$\rho C\,\frac{\partial T}{\partial t} + \mathbf{v}\,\mathrm{grad}\,T = \nabla(\kappa\,\nabla T) + W \tag{3}$$

with $\mathbf{v}$, T, ρ, C, κ velocity, temperature, density, specific heat and heat conductivity, μ viscosity of the melt, p is pressure, W is sum of volumetric energy deposition and Joule heating. The following boundary conditions are applied at the liquid vapour boundary:

$$-\kappa\left.\frac{\partial T}{\partial n}\right|_{surf} = Q(t) - \rho V_{ev}\Delta H_{ev} \tag{4}$$

$$\mu\,\frac{\partial u_y}{\partial n} = \frac{\partial \alpha}{\partial y}, \qquad \mu\,\frac{\partial u_z}{\partial n} = \frac{\partial \alpha}{\partial z}, \tag{5}$$

here in (4) temperature gradient is calculated at the surface along the normal coordinate to the surface (x-coordinate), $Q(t)$ is surface heat load, ΔH_{ev} is enthalpy of evaporation. In (5) u_y,u_z is velocity component along the surface, α is surface tension coefficient. The classic Stefan boundary condition is applied to the solid liquid boundary. At the melting front ($n = N_m$) the velocity of the melt motion assumed to be zero here n is normal to the melt front.

$$\kappa_s\left.\frac{\partial T_s}{\partial n}\right|_{n=N_m} - \kappa_l\left.\frac{\partial T_l}{\partial n}\right|_{n=N_m} = \rho V_m \Delta H_m \tag{6}$$

here index s refers to the solid and index l to the liquid phase, V_m is velocity of melting front propagation, ΔH_m is enthalpy of melting.

The "shallow water approximation" allows simplifying the system of Eqs. (1)–(3) with the boundary conditions (4)–(6) to a system of quasi 2-D equations. The fluid velocity is averaged over the melt layer thickness assuming a parabolic dependence. After averaging Eqs. (1) and (2) with the boundary condition (Eq. (5)) the system of equation is derived:

$$\frac{\partial h}{\partial t} + \frac{\partial (u_y h)}{\partial y} + \frac{\partial (u_z h)}{\partial z} = V_{ev} + V_m \tag{7}$$

$$\frac{\partial u_y}{\partial t} + u_y \frac{\partial u_y}{\partial y} = -\frac{1}{\rho}\frac{\partial p}{\partial y} - \frac{u_y}{h} V_m + \nu \frac{\partial^2 u_y}{\partial y^2} - 3\nu \frac{u_y}{h^2} + \frac{3k_\alpha}{2\rho h}\frac{\partial T}{\partial y} + \frac{J_z B_y}{\rho c} \tag{8}$$

$$\frac{\partial u_z}{\partial t} + u_z \frac{\partial u_z}{\partial z} = -\frac{1}{\rho}\frac{\partial p}{\partial z} - \frac{u_z}{h} V_m + \nu \frac{\partial^2 u_z}{\partial z^2} - 3\nu \frac{u_z}{h^2} + \frac{3k_\alpha}{2\rho h}\frac{\partial T}{\partial z} + \frac{J_y B_z}{\rho c} \tag{9}$$

Here ν is the kinematic viscosity, J_z, J_y component of the current, B_y, B_z the toroidal magnetic field components, T melt temperature, and instead of α the negative coefficient given by $k_\alpha = \partial\alpha/\partial T$ is used, V_{ev} velocity of the surface caused by the evaporation. h is the thickness of the melt layer. The equations describing the evolution of the normal velocity at the surface V_{sf} and the heat transport along the surface remain also intact:

$$V_{sf} = V_{ev} - \frac{\partial (u_y h)}{\partial y} - \frac{\partial (u_z h)}{\partial z} \tag{10}$$

$$\frac{\partial T}{\partial t} + u_y \frac{\partial T}{\partial y} + u_z \frac{\partial T}{\partial z} = \frac{3\nu}{C}\frac{u_y^2}{h^2} + \frac{3\nu}{C}\frac{u_z^2}{h^2} \tag{11}$$

To calculate the temperature field inside the target the 3D Stefan problem Eq. (3) for moving boundaries attached to re-solidification, melting and vaporization fronts is solved using the splitting method.

Temperature dependent thermo-physical data are used [10]. The model of the plasma shielding well developed, validated against experiments at plasma gun facilities, and described in details in [11] have been implemented into the code 3D MEMOS to take into account influence of the evaporated material on the surface heat loads. For 3D simulations the following simplifications were done: self-similar solution is used for estimation of the parameters of expanding vapor [9] and existing of the plasma shielding, mean charge model (by D. Post in coronal limit) is used for

the plasma ionization estimation ions contains about half of impacting energy of the ELMs plasma, mpacting ions stopping inside the expanding vapor is accounting only, heat conductivity from the plasma shielding to the wall is not accounting for, radiation from the plasma shielding to the wall is not accounting for.

4. RESULTS OF SIMULATIONS

Numerical simulations are carried out for the H-Mode JET-ILW shot JET Pulse No: 84779 with impact parameters described above for several fudge factor $f_s = 0.2, 0.3, 0.4, 0.5$, and 1.0 with and without plasma shielding accounting for. Simulation with $f_s = 1.0$ demonstrated unrealistic maximum temperatures at the ELMs exceeding 6000K and bulk melting of the special lamella during the pulse what did not observed in the experiments [4,6]. The best fitting of the experimental data (time dependences of the surface temperature, and measured vaporized tungsten) was obtained with fudge factor $f_s = 0.4$ and accounting for the plasma shielding [4,6]. Numerical simulations demonstrated that surface temperature of the leading edge is below melting point during inter ELMs time interval (Figure 3) and essentially exceeds melting point during ELMs and drops down within about several milliseconds after ELM maximum. Moreover overheated region with extremely high temperature gradients at the leading edge (~ 10^6K/m) and noticeable W evaporation is very narrow with typical scale of about several hundred microns (Figure 4a and Figure 4b). At the inter ELM time interval temperature field of the top surface of special lamella is rather smooth (Figure 4a).

Noticeable W evaporation during ELMs leads to formation of the plasma shielding in the front of the leading edge and essential screening it's from the impacting plasma leading to decreasing the surface temperature during the ELMs and preventing bulk melting at the later time moments (Figure 3). Bulk melting did not observed at any time in the experiments [4,6]. Typical melt layer thickness corresponding to the ELM maximum was about few hundred microns and final evaporation depth does not exceed 0.3 microns after 51 ElMs of JET Pulse No: 84779.

To determine main driving force responsible for the melt motion damage of special lamella observed in the JET-ILW experiments two scenarios were simulated for fudge factor 0.4 scenario with plasma shielding: A) all driving forces described above including JxB force are accounting for; and B) JxB force is excluded.

Simulations demonstrated that gradient of the plasma pressure of impacting plasma and gradient of surface tension generated melt motion with melt layer velocity of about 0.006m/s and production of final surface damage after pulse with magnitude of about 20 microns. During the ELMs the JxB force with thermo-emission current calculated in accordance with Richardson law (Figure 5) generate melt motion along leading edge in High Field Side direction with velocities up to 1.5m/s in the central molten region and up to 0.5m/s at the periphery in the direction observed experimentally (Figure 6). Such intense melt motion leads to redistribution of the molten material and producing the jet-like mountain and pattern of about 200 microns which well correlate with the observed in JET-ILW experiment ones after single pulse (Figure 7).

CONCLUSION

3D Model for multi-ELM JET-ILW experiments is implemented into MEMOS, applied for modelling shots JET Pulse No: 84514 (L-mode) and JET Pulse No: 84779 (H-mode) and verified.

MEMOS simulations for the special lamella damage are performed using different fudge factors f_s to thermal loads Qs.

The simulations for shot JET Pulse No: 84779 with fudge factor $f_s = 0.4$ and accounting for the plasma shielding appropriately fit the experimental data: time dependences of the surface temperature, and measured vaporized tungsten.

It was demonstrated that the plasma shielding play substantial role in decreasing heat loads during the ELMs. The shielding prevents bulk melting.

The JxB force with the thermo-emission current J is the main driving force of the melt motion damage.

ACKNOWLEDGEMENTS

This work, supported by the European Communities under the contract between EURATOM and KIT, was carried out within the framework of the European Fusion Development Agreement. The views and opinions expressed herein do not necessarily reflect those of the European Commission

REFERENCES

[1]. R.A. Pitts et al., 55th APS Meeting, Denver, CO, USA, paper WE1.00001;
[2]. J.W. Coenen, et al. Nuclear Fusion **51** (2011) 083008;
[3]. N. Klimov, et al., J. Nuclear Materials **415** (2011) 59.
[4]. J.W. Coenen, et al., - PSI 2014 – submitted to Journal of Nuclear Materials, (2014).
[5]. B. Bazylev and J.W. Coenen, Problems of Atomic Science and Technology 1, Series: Plasma Physics **19** (2013) 3.
[6]. G. Arnoux et al., - submitted to Journal of Nuclear Materials, (2014)
[7]. Bazylev et al., B. Physica Scripta, **T145** (2011), 014054.
[8]. Bazylev, B. et al. Journal of Nuclear Materials, **363–365** (2007), 1011–1015.
[9]. L.D. Landau, E.N. Lifshits/. Fluid Mechanics, Pergamon, New York, 1959.
[10]. Y.S. Touloukian (ed). Thermophysical Properties of Materials, New York, 1970.
[11]. H. Wuerz et al//. Fusion Science and Technology 2001, v. 40, p. 191.

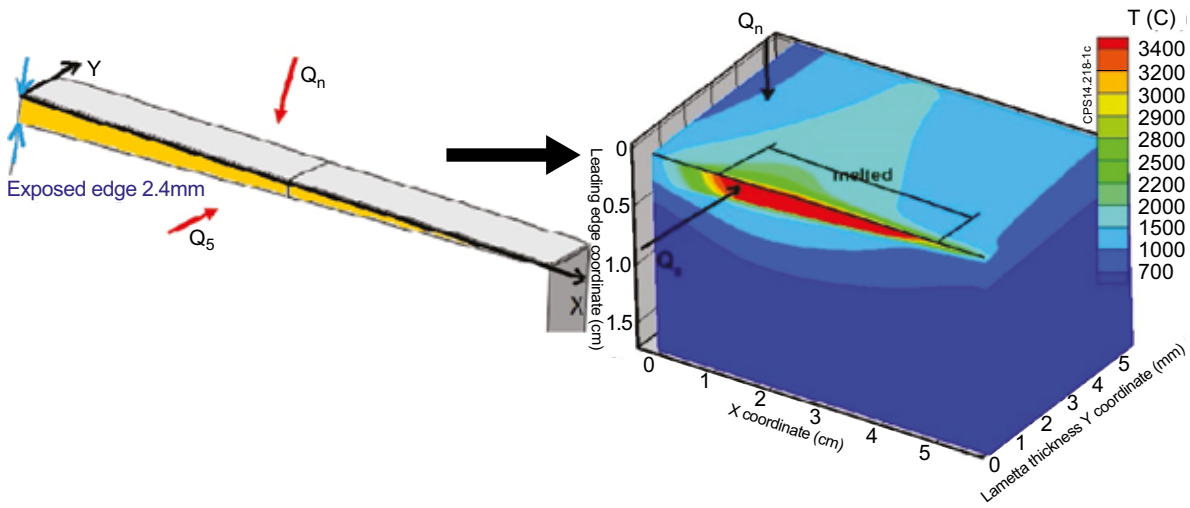

Figure 1. Sketch of Special Lamella installed in JET ILW and sketch of tungsten target used in simulation which demonstrated typical 3D temperature field at ELM maximum.

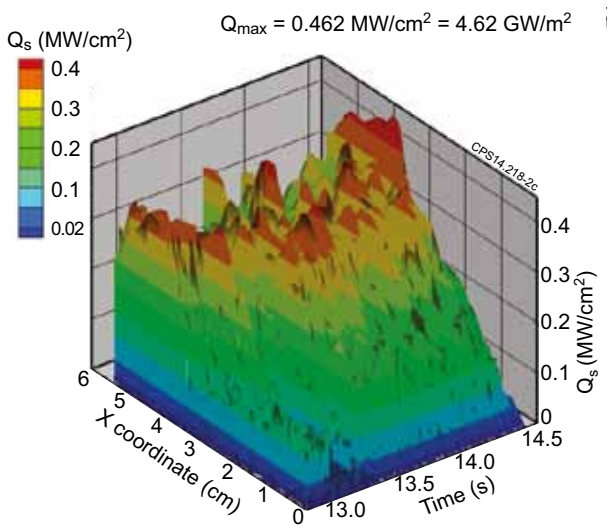

Figure 2. Time dependence of input flux Q_s along the poloidal direction (X) for the shot JET Pulse No: 84779 used in simulations.

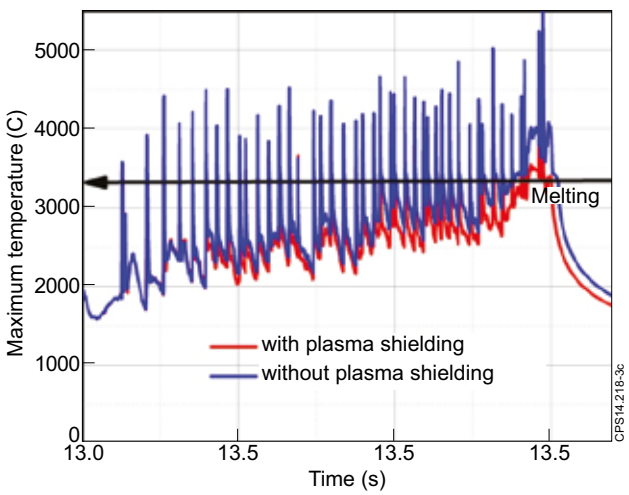

Figure 3. Time dependence of maximum of the surface temperature along leading edge of the special lamella for the shot JET Pulse No: 84779 with fudge factor $f_s = 0.4$.

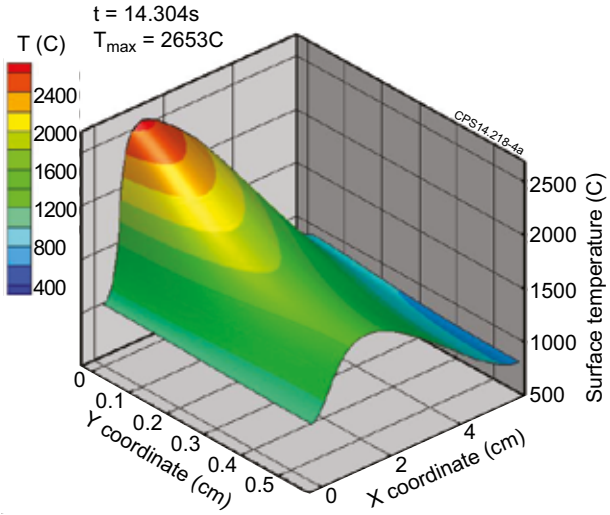

Figure 4a. Contour plots of the surface temperature at the top surface of special lamella at the inter ELMs time t = 54.304s for the shot JET Pulse No: 84779 with fudge factor f_s = 0.4.

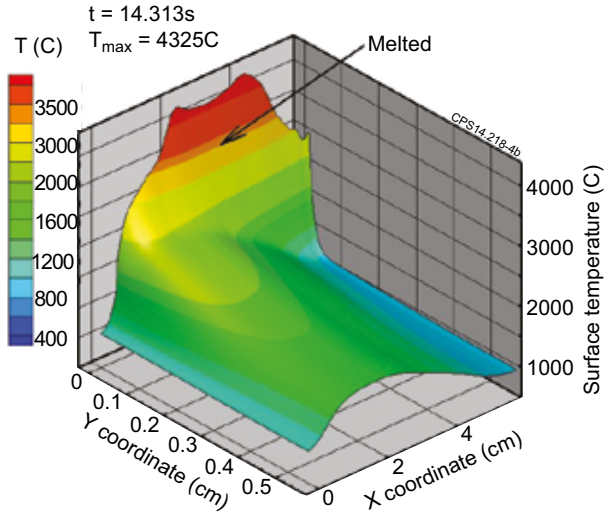

Figure 4b. Contour plots of the surface temperature at the top surface of special lamella at the time corresponding to the ELM maximum t = 54.313s for the shot JET Pulse No: 84779 with fudge factor f_s = 0.4.

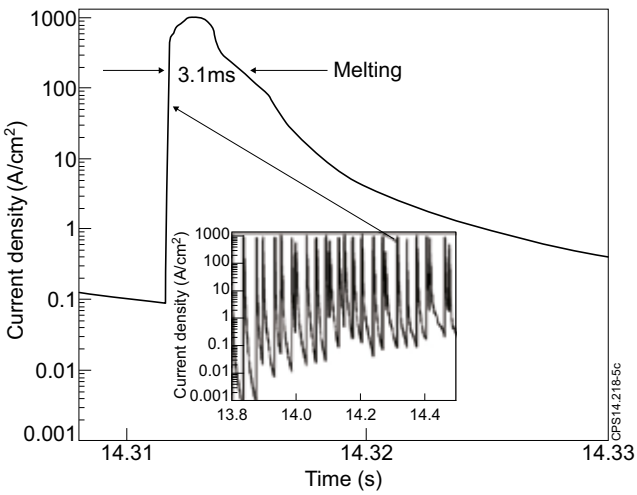

Figure 5. Time dependence of calculated mean thermo-emission current at the leading edge of the special lamella during the typical ELM for the shot JET Pulse No: 84779 with fudge factor f_s = 0.4. Figure inside demonstrates time dependence of the current for wide time interval including several tens ELMs.

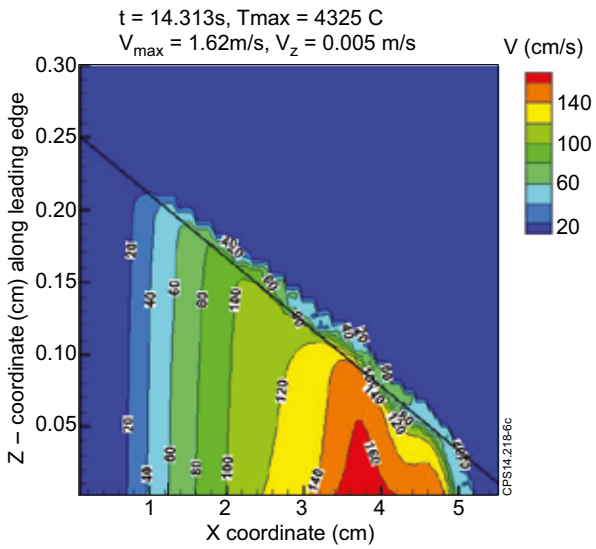

Figure 6. Contour plots of the melt layer velocity at the leading edge surface of special lamella at the time corresponding to the ELM maximum t = 54.313 s for the shot JET Pulse No: 84779 with fudge factor f_s = 0.4.

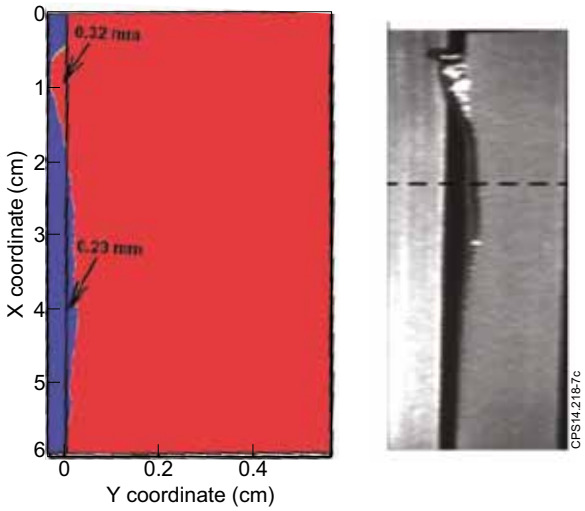

Figure 7. Final calculated surface profile view from the top surface for the shot Pulse No: 84779 factor fudge factor f_s = 0.4 (Left) and view of Specula Lamella damage (right).